



Ultrasonographic Evaluation of Liver Tissue after Surgically Induced Bile Duct Ligation in Dogs



Hiba Abdulaziz Shekho^{1*}, Ahmed Khalaf Ali² and Osamah Muwafag Al-Iraqi³

¹Department of Surgery and Obstetric, College of Veterinary Medicine, Tikrit University, Tikrit, Iraq.

²Department of Surgery and Theriogenology, College of Veterinary Medicine, University of Mosul, Mosul, Iraq.

³Department of Internal and Preventive Medicine, College of Veterinary Medicine, University of Mosul, Mosul, Iraq.

Abstract

THE current study used ultrasound to assess the induced hepatic fibrosis by ligation of common bile duct using surgical stainless-steel wire in 18 healthy local adult dogs of both sexes, weighing (20±5) kgs and aged (24±6) months. All animals were subjected to evaluated the progression of hepatic fibrosis by clinical and ultrasound examinations using a transabdominal convex transducer at frequency (5 MHz) to diagnose developing of surgically induced hepatic fibrosis at 0, 7, 14 and 21 days, respectively, after ligation of the common bile duct. Clinical results such as severe abdominal pain, anorexia, emaciation, jaundice and pale of mucus membrane were observed. Ultrasonographical examination of liver revealed dilatation of the gallbladder, common bile duct and portal vein as well as increased in thickness and echogenicity of liver tissue starting from the 7th day post-ligation till reaching the maximum in the 21 days. There was a significant difference in echogenicity of liver parenchyma between groups during the 0,7,14 and 21 days of the experiment in all dogs $p < 0.01$. In conclusion, the use of ultrasound imaging to diagnose, evaluate and follow-up the diffused liver disease models is feasible and beneficial value to monitor the development of levels and stages of hepatic fibrosis and cirrhosis of individual dogs.

Key words: Ultrasonographic examination, hepatic fibrosis, common bile duct ligation, dogs

Introduction

Hepatic fibrosis can be considered as the most typical sequel of liver damage which is a significant contributor in the development process of hepatic dysfunction, and it may result into other chronic conditions such portal hypertension [1,2]. The main characteristic feature of hepatic fibrosis is the presence of the fibrillary extracellular matrix (ECM) components which are accumulated progressively in liver [3,4]. There are changes in the collagen profile of liver tissue with increased related amounts of collagen types I and III associated with modification and cross-linking process of ECM components due to persisting inflammation [5,6]. There are certain methods to induce hepatic fibrosis by common bile duct ligation [7] is the common and safer methods which leads to an acute obstructive jaundice within two weeks and progressive

fibrosis is anticipated in approximately 4 or 6 weeks later where four weeks duration is thought to be enough to cause a moderate cell necrosis and fatty infiltration [8,9]. The actual methods for assessment of hepatic fibrosis consist of non-invasive methods based on conventional imaging methods include ultrasonography [10], computed tomography (CT)[11], and magnetic resonance imaging (MRI)[12], Newer acoustic approaches, like as transient elastography, can improve the accuracy of ultrasonography, CT, and MRI in diagnosing fibrosis or early cirrhosis [13], Acoustic radiation force impulse imaging [14], Two-dimensional shear wave elastography, Magnetic resonance elastography [15]. Ultrasonography is a more practical choice for initial diagnostic and follow-up exams since it is a safe, non-invasive, and affordable procedure that

*Corresponding author: Hiba Abdulaziz Shekho, E-mail: dr_hibashekho@tu.edu.iq, Tel.: + 9647724434469

(Received 14/12/2023, accepted 07/02/2024)

DOI: 10.21608/EJVS.2024.254677.1727

©2024 National Information and Documentation Center (NIDOC)

does not require sedation or anesthesia [16,17]. The ultrasound study protocol includes a serial imaging of liver lobes to assess certain criteria such as parenchymal echotexture, focal lesions, volumetric changes, and edge evaluation [18,19]. Following fibrosis occurrence in some parts of the liver, there are changes in ultrasound properties (absorption and reflection) [20,21]. Roughening of the liver parenchyma, thickening of the hepatic vein wall, and sharpening of the liver capsule margin are the main noticed changes [22,23].

The current study's goal was to employ ultrasound imaging system (frequency 5 MHz) to evaluate and monitor the progression of hepatic fibrosis for four intervals 0, 7, 14 and 21 days respectively after ligation of common bile duct by surgical stainless-steel wire in dogs.

Material and Methods

Experimental Animals

The experiment was carried out on 18 healthy dogs of local breed from both sexes weighing between (20±5) kgs and aged between (24±6) months. Animals of the study were kept in a place designated to house dogs belonging to the College of Veterinary Medicine, University of Mosul. These animals were treated with ivermectin at dose 0.2 mg / kg [24]. The animals were examined physically and clinically to ensure that

they are free of diseases. For adaptation, the dogs were Accommodated in animal house for 14 days before surgery.

Induction of hepatic fibrosis

This study was performed under protocol of premedication and general anesthesia including, Atropine sulphate 1% at a dose 0.04mg/Kg B.W [25], then after around 10 minutes, Ketamine (10%) and xylazine (2%) at a dose of 15mg / kg and 5 mg / kg of body weight respectively was administrated as a mixture intramuscularly [26,27]. Bile duct ligation was surgically performed in adult dogs to induce biliary obstruction [28,29]. Briefly, an incision along the midline was made in the abdominal area and the peritoneal cavity was exposed. The exposure of the common bile duct was achieved by elevating of the intestines toward the lower part of the body (Figure 1). By blunt dissection, both portal vein and accompanying hepatic artery were identified and separated from the bile duct. Surgical stainless-steel wire (1 USP) was placed around the bile duct in two places then the knots were secured by twisting. During knots tying, increasing continuous tractive force was applied to ensure effective obstruction and avoid severing of bile duct (Figure 2). The abdominal incision was then sutured in two layers.

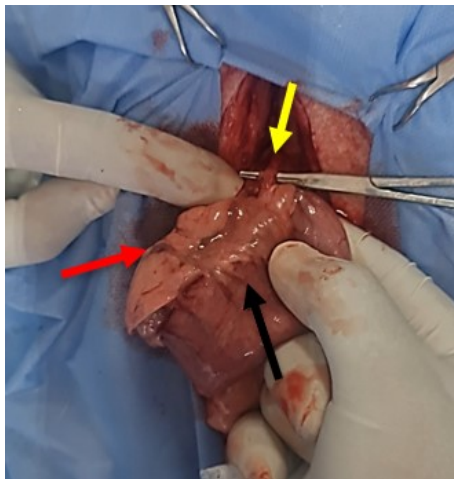


Fig. 1. Shows the anatomically normal of common bile duct (yellow arrow), duodenum (black arrow) and pancreas (Red arrow) before operation.

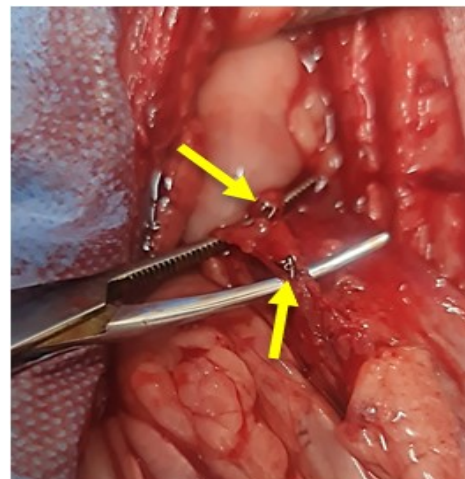


Fig. 2. Shows two surgical stainless-steel wire knots were placed around the bile duct and secured by twisting (Yellow arrow).

Postoperative examinations

The following tests were carried out for each of the experimental animal as follows:

Clinical examination

The health status of the all animals was monitored after induced of common bile duct ligation for 21 days following surgery by observing the animal's movement, activity and appetite for food.

Ultrasound examination

At the beginning, for the purpose of ensuring the integrity of the liver tissue, an ultrasonographic examination of the liver was performed for all animals using (Kaixin Kx5100vet 3,5microconvex probe Keebromed USA). After that, the common bile duct was ligated to induce hepatic fibrosis. An ultrasonographic examination was performed on the experimental dogs weekly for 21 days and the changes in the liver tissue were observed as hyperechoic and mottled heterogeneous appearance in addition to the size and thickness of the gallbladder wall, and then compared these results with the results of the initial examination obtained before the induction of fibrosis.

Statistical Analysis

The SPSS program v.23 software (SPSS In. Chicago, IL., USA) was used to do statistical analysis on the data. All data were given in the form of mean standard deviation ($\text{mean} \pm \text{S.E.}$). To evaluate if groups had significant findings, the one-

way ANOVA test was used, and P values less than 0.01 were considered significant. [30].

Results

Clinical findings

All dogs survived till the end of the study. Following ligation of common bile duct, animals suffered from severe dullness and depression, anorexia and subsequent gradual decreased body weight. Body weight was correlated negatively with corresponding cholestatic duration and Jaundice which was main sign of the dogs suffering from blockade of bile duct where yellowing of the skin, mucous membranes, and whites of the eyes was clearly noticed. Severe pain particularly during two days after surgery was observed and treated with diclofenac sodium at a dose of (1mg/kg) of body weight [31]. Food uptake improved because of progressive decrease of post-operative unease, even though still at a lesser level range resulting into progressive decrease of body weight of dogs (Figure 3).

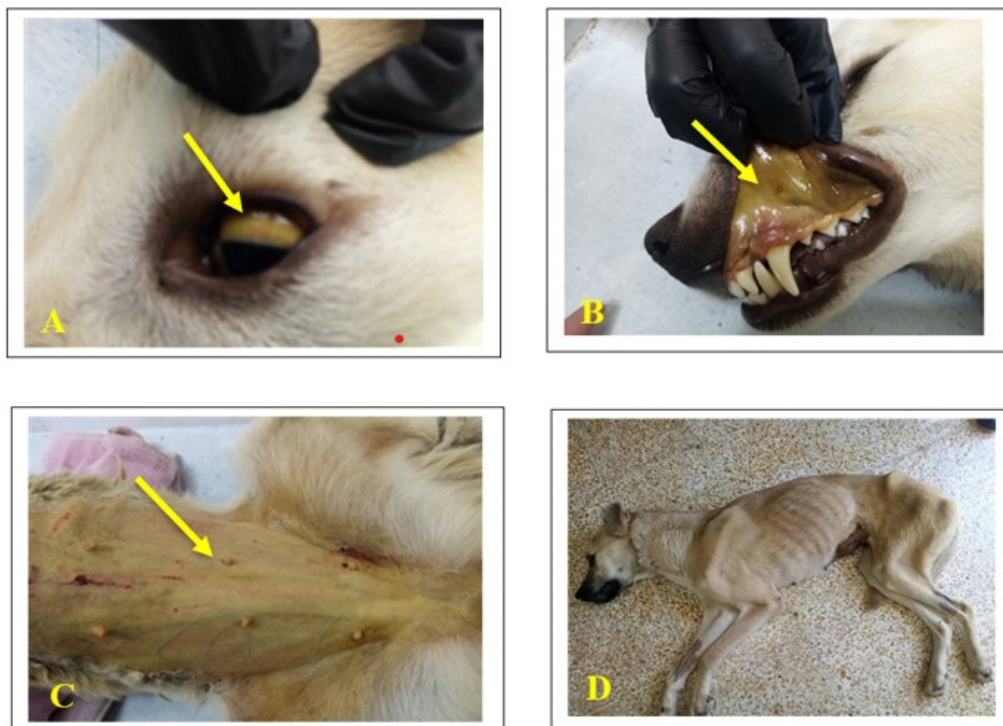


Fig.3. Shows the post-operative clinical signs. A: Yellowish mucus membrane of eye (arrow). B: Yellow oral mucus membrane (arrow). C: Yellowish skin (arrow). D. Dog suffering from cachexia.

Ultrasonographic assessment

Ultrasonography results demonstrated aberrant liver alterations in all animals, including enlargement and increase the thickness of gall bladder wall from 2mm which is the normal thickness to the 4.7mm at 21 days, as well as a mottled heterogeneous and hyperechoic appearance of the liver tissue, which replaced the typical appearance of liver tissue. These changes were

gradually observed from after the 7th day of common bile duct ligation and continued to increase until the end of the experiment (21 days), (Figures 4, 5, 6 and 7). The study's findings also revealed significant difference in a heterogeneous mottled and hyperechoic appearance of liver tissue between groups during the days of the experiment, as shown in (Table 1) and (Figure 8)

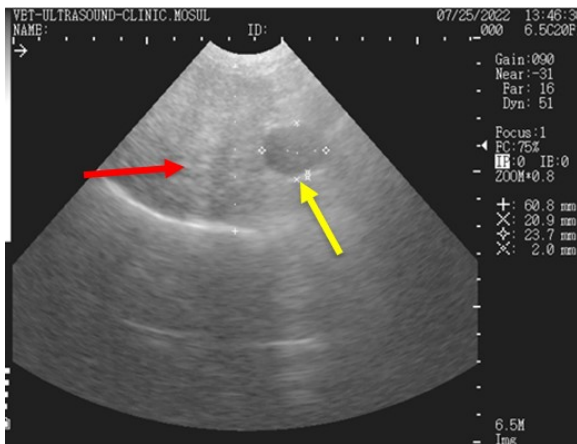


Fig. 4. Ultra-sonography at (0 day) reveals normal liver tissue (red- arrow) and normal gall bladder 2mm (yellow-arrow).

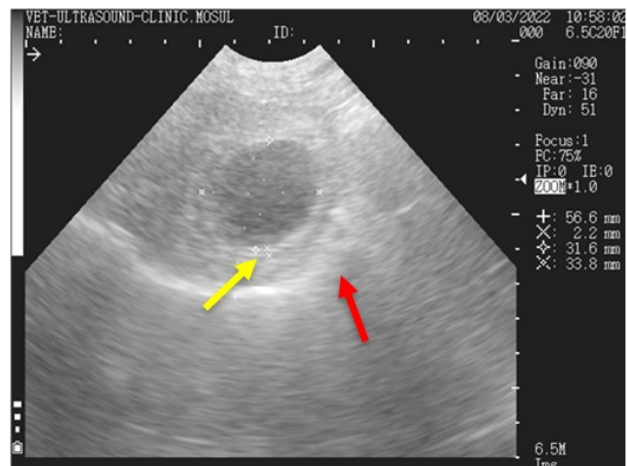


Fig. 5. Ultra-sonography at 7th postoperative day reveals heterogeneous mottled and hyperechoic appearance of liver tissue (red-arrow) and wall thickness of gall bladder 2.2 mm (yellow- arrow).

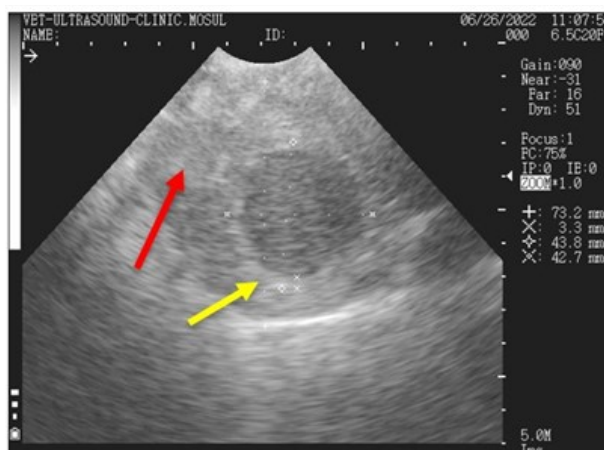


Fig. 6. Ultra-sonography at 14th postoperative day reveals increase in heterogeneous mottled appearance of liver tissue (red-arrow) and increase wall thickness and size of gall bladder 3.3mm (yellow- arrow).

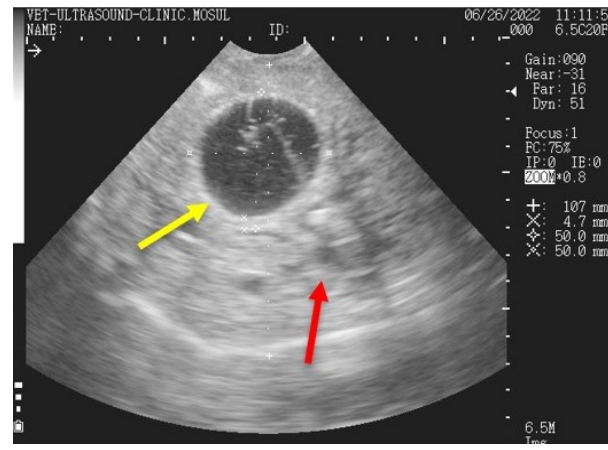


Fig. 7. Ultra-sonography at 21th postoperative day reveals sever heterogeneous mottled hyperechoic appearance of liver tissue (red-arrow) and increase wall thickness and size of gall bladder 4.7mm (yellow -arrow).

Table 1. Significant difference in heterogeneous mottled and hyperechoic appearance of liver tissue between groups during the days of the experiment

Groups	Heterogeneous mottled and hyperechoic appearance of liver tissue
	Mean ± SE
0 day	68.8 ± 3.267 ^a
7 days	79.7 ± 6.003 ^b
14 days	88.6 ± 2.769 ^{bc}
21 days	95.7 ± 2.093 ^c

Small different litters mean significant differences between groups at p<0.01

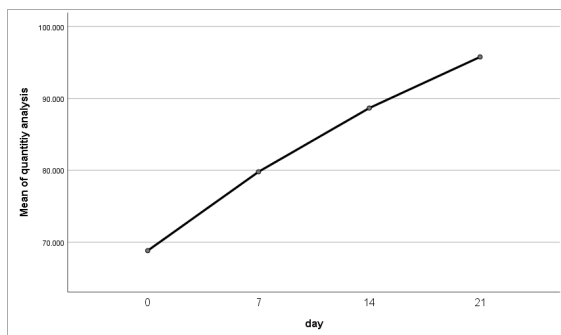


Fig.8. Showed that there were gradually increases in a heterogeneous mottled and hyperechoic appearance of liver tissue between groups during the days of the experiment.

Discussion

In this study, dogs who underwent experimental common bile duct ligation with surgical stainless-steel wire developed cholestasis two days after the procedure. The first noticed symptom in all animals was jaundice, which could be attributed to an increased bilirubin levels in blood due to impaired flow of bile following ligation of the duct and subsequent deposition of this agent in tissues, primarily in the skin as well as mucous membranes. These results are similar to those obtained by Bayoumi *et.al* and Vardar *et al.*[32,33] . Long-term occlusion of the bile duct decreases enterohepatic circulation causing the feces to turn clay-colored, and shifts the kidney's role as the primary site for bilirubin clearance, which changes the urine color into orange [34,35]. could all be attributed to, which causes hepatic bile salts retention and the subsequent severe destruction of the hepatocytes are caused by the impaired flow of bile within extrahepatic biliary tree resulting into abdominal pain, extreme emaciation, diarrhea, decreased appetite and weight loss. In the current study, the

animals showed various degrees of hepatic dysfunction, and these results were in accordance with previous study conducted by Otte *et al.* and Gomaa *et.al.* [36,37].

Post-operative pain is particularly severe during the first two days following the surgical ligation of common bile duct, as this condition can lead to enlargement of the liver, which causes abdominal pain, actually, the liver doesn't contain nerves, so the organ itself can't feel pain. Even so, the sensation of liver pain can occur because the layer of tissue that surrounds the organ called Glisson's Capsule does contain nerves. Any diseases affecting the liver that increase its size can result in what feels like liver pain, as the enlarged liver presses on its outer capsule this sign has been proven by [38].

In our experimental study, the outcomes of the ultrasonography revealed abnormal changes of the hepatic tissue in all of the animals like increased gallbladder size and its wall thickness from the normal of 2 mm to 4.7 mm as well as a mottled heterogeneous and hyperechoic appearance of the liver tissue typical appearance of liver tissue, and these outcomes matched those of earlier study had carried out by [39]. All animals underwent these alterations which were visible 7 days after ligation of common bile duct and endured with progressively increased till the end of the experiment, so that they appeared more clearly 21 days after inducing fibrosis. The significance of ultrasonographic examination in detecting and evaluating abnormalities in liver tissue linked to hepatic echoes and nodularity in dogs with mild to severe fibrosis was observed by Bataller and Brenner; Endo *et al.* and Vidal-González *et.al.* [40,41,42] who supported the use of ultrasound to diagnose hepatic fibrosis and cirrhosis.

Conclusion

Ligation of common bile duct with surgical stainless-steel wire was highly effective in inducing liver fibrosis and the use of ultrasonographical examination in extrahepatic cholestasis was crucial in the early detection of the obstruction and identification of the changes that occurred within two days following common bile duct ligation.

Conflict of interest

The authors state that they have no conflicts of interest.

Ethical approve

The present study has been given approval by the Institutional Animal Care and Use committee of the College of Veterinary Medicine, University of Mosul (UM.VET.2021.026).

Funding statement

The funding into the research was funded by the authors.

Acknowledgements

The authors are grateful to College of Veterinary Medicine, Mosul University for providing the laboratory facilities.

Authors Contribution

The authors each contributed equally.

References

- Toosi, A. E. K. Liver Fibrosis: Causes and Methods of Assessment, A Review. *Romanian Journal of Internal Medicine*, **53**(4), 304–314 (2015). <https://doi.org/10.1515/rjim-2015-0039>
- Brol, M. J., Drebber, U., Luetkens, J. A., Odenthal, M. and Trebicka, J. The pathogenesis of hepatic fibrosis: basic facts and clinical challenges—assessment of liver fibrosis: a narrative review. *Digestive Medicine Research*, **5**(4), 24–24 (2022). <https://dx.doi.org/10.21037/dmr-22-9>.
- Ortiz, C., Schierwagen, R., Schaefer, L., Klein, S., Trepap, X. and Trebicka, J. Extracellular Matrix Remodeling in Chronic Liver Disease. *Current Tissue Microenvironment Reports*, **2**(3), 41–52 (2021). <https://doi.org/10.1007/s43152-021-00030-3>.
- Khalil, M. H., Ali, A. K. and Al-Iraqi, O. M. New surgical model to induce irreversible liver fibrosis by surgical closure of major duodenal orifice in dogs. *Iraqi Journal of Veterinary Sciences*, **36**(3), 825–831(2022). <https://doi.org/10.33899/ijvs.2022.132219.2071>.
- Eulenberg, V. M. and Lidbury, J. A. Hepatic Fibrosis in Dogs. *Journal of Veterinary Internal Medicine*, **26**–41(2018). <https://doi.org/10.1111/jvim.14891>.
- McQuitty, C. E., Williams, R., Chokshi, S. and Urbani, L. Immunomodulatory Role of the Extracellular Matrix Within the Liver Disease Microenvironment. *Frontiers in Immunology*, **11**, 1–33(2020). <https://doi.org/10.3389/fimmu.2020.574276>.
- Ozozan, O. V., Dinc, T., Vural, V., Ozogul, C., Ozmen, M. M. and Coskun, F. An electron microscopy study of liver and kidney damage in an experimental model of obstructive jaundice. *Ann. Ital. Chir.*, **91**(1), 122–130(2020). www.annitalchir.com
- Marques, T. G., Chaib, E., da Fonseca, J. H., Lourenço, A. C. R., Silva, F. D., Ribeiro, M. A. F., Galvão, F. H. F. and Augusto Carneiro, L. Review of experimental models for inducing hepatic cirrhosis by bile duct ligation and carbon tetrachloride injection. *Acta Cirurgica Brasileira*, **27** (8), 589 (2012). www.researchgate.net/publication/237836476_Experimental_model_for_inducing_cirrhosis
- Martinez-Lopez, S., Angel-Gomis, E., Sanchez-Ardid, E., Pastor-Campos, A., Picó, J. and Gomez-Hurtado, I. The 3Rs in Experimental Liver Disease. *Animals*, **13**(14), 1–32 (2023). <https://doi.org/10.3390/ani13142357>.
- Zhang, Y. N., Fowler, K. J., Ozturk, A., Potu, C. K., Louie, A. L., Montes, V., Henderson, W. C., Wang, K., Andre, M. P., Samir, A. E. and Sirlin, C. B. Liver fibrosis imaging: A clinical review of ultrasound and magnetic resonance elastography. *Journal of Magnetic Resonance Imaging*, **51**(1), 25–42 (2020). <https://doi.org/10.1002/jmri.26716>.
- Wang, J. C., Fu, R., Tao, X. W., Mao, Y. F., Wang, F., Zhang, Z. C., Yu, W. W., Chen, J., He, J. and Sun, B. C. A radiomics-based model on non-contrast CT for predicting cirrhosis: Make the most of image data. *Biomarker Research*, **8**(1), 1–12 (2020). <https://doi.org/10.1186/s40364-020-00219-y>
- Alnimer, L. and Nouredin, M. Non-invasive imaging biomarkers for liver steatosis in non-alcoholic fatty liver disease: present and future. *Clinical and Molecular Hepatology*, **29**(2), 2–6 (2023). <https://doi.org/10.3350/cmh.2023.0104>
- Yu, J. H., Lee, H. A. and Kim, S. U. Noninvasive imaging biomarkers for liver fibrosis in nonalcoholic fatty liver disease: current and future Jung. *Clinical and Molecular Hepatology*, **29**(2), 394–397(2023). <https://doi.org/10.3350/cmh.2022.0436>
- da Silva, R. G. Junior, de Miranda, M. L. Q., de Araújo Caldeira Brant, P. E., Schulz, P. O., de Fátima Araujo Nascimento, M., Schmillevitch, J., Vieira, A., de Freitas, W. R. Junior and Szutan, L. A. Acoustic radiation force impulse elastography and liver fibrosis risk scores in severe obesity. *Arch. Endocrinol. Met. Ab.*, **65**(6), 730–738 (2021). <https://doi.org/10.20945/2359-399700000397>.
- Wang, Y., Shi, K., Tu, J., Ke, C., Chen, N., Wang, B., Liu, Y. and Zhou, Z. Atractylenolide III Ameliorates Bile Duct Ligation-Induced Liver Fibrosis by Inhibiting the PI3K/AKT Pathway and Regulating Glutamine Metabolism. *Molecules (Basel, Switzerland)*, **28**(14), 5504(2023). <https://doi.org/10.3390/molecules28145504>.
- Allawi, A. H., Alkattan, L. M. and Al Iraqi, O. M. Clinical and ultrasonographic study of using autogenous venous graft and platelet-rich plasma for repairing Achilles tendon rupture in dogs. *Iraqi Journal of Veterinary Sciences*, **33**(2), 453–460 (2019). <https://doi.org/10.33899/ijvs.2019.163199>.
- Villani, R., Lupo, P., Sangineto, M., Romano, A. D. and Serviddio, G. Liver Ultrasound Elastography in Non-Alcoholic Fatty Liver Disease: A State-of-the-Art Summary. *Diagnostics*, **13**(7), 1236 (2023). <https://doi.org/10.3390/diagnostics13071236>.
- Choong, C. C., Venkatesh, S. K. and Siew, E. P. Y. Accuracy of Routine Clinical Ultrasound for Staging of Liver Fibrosis. *Journal of Clinical Imaging Science*, **2**(3), 58 (2012). <https://doi.org/10.4103/2156-7514.101000>.

19. Huang, K., Li, Q., Zeng, W., Chen, X., Liu, L., Wan, X., Feng, C., Li, Z., Liu, Z. and Dong, C. Ultrasound score combined with liver stiffness measurement by sound touch elastography for staging liver fibrosis in patients with chronic hepatitis B: a clinical prospective study. *Annals of Translational Medicine*, **10**(6),271–271(2022). <https://doi.org/10.21037/atm-22-505>.
20. Xue, L. Y., Jiang, Z. Y., Fu, T. T., Wang, Q. M., Zhu, Y. L., Dai, M., Wang, W. P., Yu, J. H. and Ding H. Transfer learning radiomics based on multimodal ultrasound imaging for staging liver fibrosis. *European Radiology*, **30**(5), 2973–2983 (2020). <https://doi.org/10.1007/s00330-019-06595-w>.
21. Cloutier, G., Destrempes, F., Yu, F. and Tang, A., Quantitative ultrasound imaging of soft biological tissues: a primer for radiologists and medical physicists. *Insights into Imaging*, **12**(127), (2021). <https://doi.org/10.1186/s13244-021-01071-w>.
22. Xie, Y., Chen, S., Jia, D., Li, B., Zheng, Y. and Yu, X. Artificial Intelligence-Based Feature Analysis of Ultrasound Images of Liver Fibrosis. *Computational Intelligence and Neuroscience*. **2022** (2859987) (2022). <https://doi.org/10.1155/2022/2859987>.
23. Singh, S., Hoque, S., Zekry, A. and Sowmya, A. Radiological Diagnosis of Chronic Liver Disease and Hepatocellular Carcinoma: A Review. *Journal of Medical Systems*, **47**(73) (2023). <https://doi.org/10.1007/s10916-023-01968-7>.
24. Abdulmawjood, Y. F., Thanoon, M G., Ibrahim, S. M. and Alsofy, J. H. Histopathological study about the effect of nano magnesium oxide and platelets rich fibrin on the healing of induced radial fracture in dogs. *Iraqi Journal of Veterinary Sciences*, **36**(suppl), 123–130 (2022). <https://doi.org/10.33899/ijvs.2022.135761.2516>.
25. Abdulmawjood, Y. F. and Thanoon, M. G. A comparative study of nano magnesium oxide versus platelets rich fibrin to repair the induced radial fracture in dogs. *Iraqi Journal of Veterinary Sciences*, **36**(2), 451–458(2022). <https://doi.org/10.33899/ijvs.2021.130500.1836>.
26. Mohammed, F. M., Alkattan, L. M. and Ismail, H. K. Histopathological and serological assessment of using rib lamb xenograft reinforced with and without hydroxyapatite nano gel for reconstruction tibial bone defect in dogs. *Iraqi Journal of Veterinary Sciences*, **36**, 69–76 (2022). <https://doi.org/10.33899/ijvs.2022.135366.2473>.
27. Raffea, N. M. and Allawi, A. H. Effect of autologous peritoneum and platelet-rich fibrin graft on healing of intestinal anastomosis in dogs. *Iraqi Journal of Veterinary Sciences*, **36**(2), 459–470 (2022). <https://doi.org/10.33899/ijvs.2021.130529.1840>.
28. Tag, C. G., Sauer-Lehnen, S., Weiskirchen, S., Borkham-Kamphorst, E., Tolba, R. H., Tacke, F. and Weiskirchen, R. Bile duct ligation in mice: Induction of inflammatory liver injury and fibrosis by obstructive cholestasis. *Journal of Visualized Experiments*, (96), 52438 (2015). <https://doi.org/10.3791/52438>.
29. Wang, J., Sun, J., Qin, T., Ren, X., Zhang, J. and Lu, X. Liver fibrosis from viral hepatitis: advances in non-invasive diagnosis. *Cancer Insight*, **2**(1), 9–30 (2023). <https://doi.org/10.58567/ci02010002>.
30. McCormick, K. and Salcedo, J. SPSS statistics for data analysis and visualization. USA: John Wiley and Sons. 275-302 (2017).
31. Abu-Seida, A.M.A. Efficacy of diclofenac sodium, either alone or together with cefotaxime sodium, for control of postoperative pain, in dogs undergoing ovariohysterectomy. *Asian Journal of Animal and Veterinary Advances*, **7**(2),180–186 (2012). <https://doi.org/10.3923/ajava.2012.180.186>
32. Bayoumi, Y., Metwally, E., El Nagar, E., Abdel Razik, W., El Seddawy, N. and Gomaa, M. Hepatorenal Syndrome in Dogs with Experimental Extrahepatic Cholestasis. *Zagazig Veterinary Journal*. **48**(1), 12–22 (2020). <https://doi.org/10.21608/zvjz.2019.15292.1068>.
33. Vardar, B. U., Dupuis, C. S., Goldstein, A. J., Vardar, Z. and Kim, Y. H. Ultrasonographic evaluation of patients with abnormal liver function tests in the emergency department. *Ultrasonography*, **41**(2),243-262 (2022). <https://doi.org/10.14366/usg.21152>.
34. Wang, L. and Wei Feng, Y., Obstructive jaundice and perioperative management. *Acta Anaesthesiologica Taiwanica.*, **52**(1), 22–29 (2014). <https://doi.org/10.1016/j.aat.2014.03.002>.
35. Vagholkar, K. Obstructive Jaundice: Understanding the pathophysiology. *International Journal of Surgery and Medicine*. **6**(0), 1(2020). <https://doi.org/10.5455/ijsm.2020-07-061-jaundice>.
36. Otte, C. M. A., Penning, L. C. and Rothuizen, J. Feline biliary tree and gallbladder disease: Aetiology, diagnosis and treatment. *Journal of Feline Medicine and Surgery*, **19**(5), 514–528(2017). <https://doi.org/10.1177/1098612X17706465>.
37. Gomaa, M., Metwally, E., El Nagar, E A., Razik, W. A., El Seddawy, N. and Bayoumi, Y. Experimental extrahepatic cholestasis in dogs: Ultrasonographic, biochemical and histopathological study. *Advances in Animal and Veterinary Sciences*, **7**(2), 44–50 (2019). <https://doi.org/10.17582/JOURNAL.AAVS/2019/7.S2.44.50>.
38. Hamilton, J. Pain Management in Liver Disease. *Gastroenterology & Hepatology* **19**(6), 355–358 (2023)
39. Khammas, A.S. and Mahmud, R. Ultrasonographic measurements of the liver, gallbladder wall thickness, inferior vena cava, portal vein and pancreas in an Urban Region, Malaysia. *Journal of Medical Ultrasound*, **29**(1), 26–31(2021). https://doi.org/10.4103/JMU.JMU_53_20.

40. Bataller, R. and Brenner, D. A. Liver fibrosis. *Journal of Clinical Investigation*, **115**(2), 209–218(2005). <https://doi.org/10.1172/JCI24282>.
41. Endo, M., Soroida, Y., Sato, M., Kobayashi, T., Hikita, H., Sato, M., Gotoh, H., Iwai, T., Sone, S., Sasano, T., Sumi, Y., Koike, K., Yatomi, Y. and Ikeda, H. Ultrasound evaluation of liver stiffness: Accuracy of ultrasound imaging for the prediction of liver cirrhosis as evaluated using a liver stiffness measurement. *Journal of Medical and Dental Sciences*, **64**(2–3), 27–34(2017). <https://doi.org/10.11480/jmds.640301>.
42. Vidal-González, D., Uribe, M., Montalvo-Javé, E. E. and Nuño-Lámbarri, N. Assessment of non-alcoholic fatty liver disease by non-invasive methods: present and future perspectives. *Revista Médica del Hospital General de Mexico*, **83**(3), 135–143(2020). <https://doi.org/10.24875/hgm.20000088>.

تقييم تليف الكبد المستحدث جراحيا في الكلاب عن طريق ربط القناة الصفراوية الرئيسية باستخدام الموجات فوق الصوتية

هبة عبدالعزيز شيخو¹، احمد خلف علي² واسامة موفق العراقي³

¹ فرع الجراحة والتوليد - كلية الطب البيطري - جامعة تكريت - صلاح الدين - العراق.

² فرع الجراحة وعلم تناسل الحيوان - كلية الطب البيطري - جامعة الموصل - الموصل - العراق.

³ فرع الطب الباطني والوقائي - كلية الطب البيطري - جامعة الموصل - الموصل - العراق.

الخلاصة

استخدمت الدراسة الحالية الموجات فوق الصوتية لتقييم تليف الكبد المستحدث عن طريق ربط القناة الصفراوية الرئيسية باستخدام سلك معدني في 18 كلباً بالغاً محلياً سليماً من كلا الجنسين تراوحت أوزانها (15-25) كجم وأعمارها (6-36) شهراً. تم إخضاع جميع الحيوانات لتقييم تطور تليف الكبد عن طريق الفحوصات السريرية والموجات فوق الصوتية باستخدام محول محدد عبر البطن بتردد (5 ميغا هرتز) لتقييم التليف قبل ربط القناة لمعرفة الحالة الصحية للحيوانات. تم فحص الحيوانات بالموجات فوق الصوتية لمدة ثلاث فترات عند 7 و 14 و 21 يوماً على التوالي بعد ربط القناة الصفراوية المشتركة. تمت ملاحظة عدد من النتائج السريرية مثل آلام البطن وفقدان الشهية والهزال واليرقان وشحوب الغشاء المخاطي. كشف التصوير بالموجات فوق الصوتية للكبد عن تضخم المرارة والقناة الصفراوية المشتركة والوريد البابي بالإضافة إلى زيادة في سماكة أنسجة الكبد وصدئها بدءاً من اليوم السابع بعد الربط حتى الوصول إلى الحد الأقصى في 21 يوماً. كان هناك اختلاف معنوي في سماكة أنسجة الكبد وصدئها بين المجموعات (0 و 7 و 14 و 21 يوماً من التجربة لدى جميع الكلاب يمكن الاستنتاج إن استخدام التصوير بالموجات فوق الصوتية لتشخيص ومتابعة العديد من أمراض الكبد المنتشرة أمر ممكن وفعال لمراقبة تطور مستويات ومرحل تليف الكبد لدى الكلاب.

الكلمات المفتاحية: الفحص بالموجات فوق الصوتية، تليف الكبد، ربط القناة الصفراوية المشتركة، الكلاب.